

ESD-TR-67-427  
ESTI FILE COPY

# ESD RECORD COPY

ESD-TR-67-427

RETURN TO  
SCIENTIFIC & TECHNICAL INFORMATION DIVISION  
(ESTI), BUILDING 1211

MTR-488

## ESD ACCESSION LIST

ESTI Call No. **59520**

Copy No.      of      cys.

EFFECT OF RADAR SYSTEM INCOHERENCE ON ACHIEVABLE  
MAINLOBE WIDTHS AND SIDELobe LEVELS

FEBRUARY 1968

J. T. Lynch

Prepared for  
DEVELOPMENT ENGINEERING DIVISION  
DIRECTORATE OF PLANNING AND TECHNOLOGY  
ELECTRONIC SYSTEMS DIVISION  
AIR FORCE SYSTEMS COMMAND  
UNITED STATES AIR FORCE  
L. G. Hanscom Field, Bedford, Massachusetts



This document has been approved for public  
release and sale; its distribution is un-  
limited.

Project 7150  
Prepared by  
THE MITRE CORPORATION  
Bedford, Massachusetts  
Contract AF19(628)-5165

ADDoc 429

When U.S. Government drawings, specifications, or other data are used for any purpose other than a definitely related government procurement operation, the government thereby incurs no responsibility nor any obligation whatsoever; and the fact that the government may have formulated, furnished, or in any way supplied the said drawings, specifications, or other data is not to be regarded by implication or otherwise, as in any manner licensing the holder or any other person or corporation, or conveying any rights or permission to manufacture, use, or sell any patented invention that may in any way be related thereto.

Do not return this copy. Retain or destroy.

EFFECT OF RADAR SYSTEM INCOHERENCE ON ACHIEVABLE  
MAINLOBE WIDTHS AND SIDELobe LEVELS

FEBRUARY 1968

J. T. Lynch

Prepared for  
DEVELOPMENT ENGINEERING DIVISION  
DIRECTORATE OF PLANNING AND TECHNOLOGY  
ELECTRONIC SYSTEMS DIVISION  
AIR FORCE SYSTEMS COMMAND  
UNITED STATES AIR FORCE  
L. G. Hanscom Field, Bedford, Massachusetts



This document has been approved for public release and sale; its distribution is unlimited.

Project 7150  
Prepared by  
THE MITRE CORPORATION  
Bedford, Massachusetts  
Contract AF19(628)-5165

## FOREWORD

The work reported in this document was performed by The MITRE Corporation, Bedford, Massachusetts, for the Development Engineering Division, Directorate of Planning and Technology, Electronic Systems Division, of the Air Force Systems Command under Contract AF 19(628)-5165.

## REVIEW AND APPROVAL

Publication of this technical report does not constitute Air Force approval of the report's findings or conclusions. It is published only for the exchange and stimulation of ideas.

A handwritten signature in black ink, reading "Anthony P. Trunfio". The signature is fluid and cursive, with the first name "Anthony" being more prominent and the last name "Trunfio" following in a similar style.

ANTHONY P. TRUNFIO, Technical Advisor  
Development Engineering Division  
Directorate of Planning and Technology

## ABSTRACT

The loss in radar resolution, that is, the increase in mainlobe width and sidelobe level, has been computed for signals corrupted by a stationary random phase process. By making approximations appropriate to a coherent radar, an easily interpreted analysis is possible. The application to a CW radar or a pulsed radar using a reference oscillator with broadband phase errors is straightforward and indicates that a hash sidelobe level is introduced. A more general application, which corresponds to a crystal oscillator reference with narrowband phase errors requires the calculation of a convolution. Hash sidelobes are introduced in this case also, except that their level is a simple function of the ratio of the phase error and signal bandwidth.

#### ACKNOWLEDGMENT

The work presented in this paper has been guided by Ron Haggarty. Gerry O'Leary deserves special mention because we worked so closely on all of the material. Ron's and Gerry's ideas so completely permeate the work that individual references have not been possible. The programming and mathematical backup work of Paul Gleason and the contribution of David Kramer is greatly appreciated.

## TABLE OF CONTENTS

	<u>Page</u>
LIST OF ILLUSTRATIONS	vi
SECTION I      INTRODUCTION TO SYSTEM COHERENCE	1
CONCLUSIONS	3
SECTION II      CALCULATION OF TRANSMIT SIGNAL SPECTRUM	6
SECTION III     EFFECT OF FINITE DELAY	11
SECTION IV      APPLICATIONS AND NUMERICAL EXAMPLES	15
CASE A   PULSED RADAR - MICROWAVE OSCILLATOR	15
CASE B   CW RADAR	18
CASE C   PULSED RADAR - CRYSTAL OSCILLATOR	21
SECTION V      SUMMARY	33
APPENDIX       CALCULATION OF SPECTRA OF PULSED RANDOM PROCESS	37
REFERENCES	48
BIBLIOGRAPHY	49

# LIST OF ILLUSTRATIONS

<u>Figure Number</u>		<u>Page</u>
1	Relationship of Radar Signals	12
2	Spectrum of Received Signal Case A - Wide Band Phase	17
3	Spectrum of Received Signal Case B - CW Radar	20
4	Received Signal Power Spectrum - CW Signal	22
5	Received Signal Power Spectrum	25
6	Received Signal Power Spectrum	27
7	Received Signal Power Spectrum	28
8	Received Signal Power Spectrum	29
9	Received Signal Power Spectrum	30
10	Sidelobe Level $\left[ \mathcal{L}_R\left(\frac{4.5}{T}\right) \right]$ vs $\Omega T$	31



## SECTION I

### INTRODUCTION TO SYSTEM COHERENCE

A radar system using frequency measurements to estimate target velocity is in some sense coherent. That is, phase as a function of time is used to provide resolution in the frequency domain. The phase information is used to increase the energy in some frequency band while attenuating it in some other band. The resolution can be measured by the width of the main lobe region (main lobe width) and the level of the cleared region (sidelobes). If the phase information has deviations from the proper structure, the system performance in terms of main lobe width and sidelobe level will be degraded.

Phase information can also be used to give angular or range resolution. Angular resolution is achieved by measuring phase information as a function of distance along an array, while range resolution is achieved by measuring phase information as a function of frequency. The mathematics of each of these problems is the same. Therefore, the application of the analysis presented in this paper applies to range and angular resolution problems as well as doppler resolution. Consequently, much of the work done on phase error effects has appeared in the literature on antennas.

The phase errors may be deterministic or random. Deterministic phase errors can often be modeled by a few terms of a power series or a few terms of a Fourier series (periodic or quadratic, etc.). For these cases, the degradation can be described analytically or

calculated in a straightforward manner on a digital computer.<sup>[1]</sup>

Random phase errors may have varying statistics (non-stationary) or constant statistics (stationary). An example of a non-stationary random phase process is random frequency modulation. Even if the frequency random process is stationary, the phase process is not. Stationary random processes are easier to describe. They model many phenomena including oscillator short-term instability, additive noise, propagation media inhomogeneities or variations, random target motion, and antenna distortion or vibration. A bibliography of relevant papers is compiled at the end of this report. Oscillator instability and its effects has received the most attention.<sup>[2]</sup>

This paper is an extension of the paper by Raven<sup>[3]</sup> in that issue of the Proceedings in which he develops a quantitative description of the effects of stationary phase errors. The analysis is applied to oscillator incoherence (phase errors vs time) and its effects on doppler resolution and sidelobes. Raven's work is extended to include the effects of short pulse length (a common radar situation). These results are applied to state-of-the-art equipment (good oscillator stability and low expected sidelobe level). This makes it easy to interpret the results and gain insight into the distortion mechanisms and to determine state-of-the-art radar capability.

Two outstanding papers on the effects of random phase errors have appeared in the literature on antenna design. A thesis by Ruze<sup>[4]</sup> presents an analysis for computing the variance of the sidelobes for

a discrete array or for a continuous array where the correlation interval is small relative to the array length. This rigorous analysis is valid for a stationary gaussian random phase process with no restriction on the variance of the phase errors. A paper by Develet<sup>[5]</sup> emphasizes the loss in resolution as a result of random phase errors. A gaussian correlation function is assumed ( $R(\tau) \approx e^{-\alpha|\tau|^2}$ ) but no restriction is placed on the correlation interval or the phase process variance. Graphs of the RMS antenna pattern are provided for a wide range of correlation intervals and RMS phase errors. These graphs also indicate the loss in sidelobe level.

The analysis in both these papers is rigorous but, therefore, very complicated. By treating only phase processes with a small RMS level, it is possible to determine the loss in main lobe width and sidelobe level for an arbitrary correlation function. This approach, which is taken in this paper, offers more insight into the degradation mechanisms.

## CONCLUSIONS

The results of the analysis are

- (1) The spectrum of the transmit signal  $\mathcal{S}_T(f)$  is given

by

$$\mathcal{S}_T(f) = [\mu_o(f) + \mathcal{S}_\phi(f)] \otimes S_I^2(f) \quad (1)$$

### Note on Notation:

Lower case s is a voltage vs time  $s(t)$

Upper case S is a voltage vs frequency,  $S(f)$  is a signal spectrum

Script  $\mathcal{S}$  is [voltage]<sup>2</sup> vs frequency,  $\mathcal{S}(f)$ , is a power spectrum

Upper case R is [voltage]<sup>2</sup> vs time delay,  $R(\tau)$ , is a correlation function

The subscript I refers to an ideal uncorrupted signal  $s_I(t)$ ,  $S_I(f)$

where  $S_I(f)$  is the frequency characteristic of the uncorrupted signal,  $\mathcal{J}_\phi(f)$  is the power spectral density of the stationary phase process and where the symbol  $\otimes$  denotes a convolution.

(2) The spectrum of the coherently demodulated received signal differs from the transmit signal only in one aspect. The phase process becomes a phase difference process  $[\Delta\phi(t)]$  with spectral density

$$\mathcal{J}_{\Delta\phi}(f) = 2 \mathcal{J}_\phi(f) [1 - \cos 2\pi f T_d] \quad (2)$$

where  $T_d$  is the round trip propagation delay. Therefore<sup>\*</sup>

$$\mathcal{J}_R(f) = [\mu_o(f) + 2 \mathcal{J}_\phi(f) [1 - \cos 2\pi f T_d]] \otimes |S_I(f)|^2$$

The applications of the analysis to practical radar situations are:

(A) If a microwave oscillator is used as the coherent reference in a pulsed radar, then the spectrum of the phase process ( $\Omega$ ) is wider than the signal spectrum ( $\Omega > \frac{1}{T}$ ). If the delay time is greater than the pulse length,  $[T_d > T]$ , the spectrum of the received signal is

$$\mathcal{J}_R(f) = |S_I(f)|^2 + 4 \mathcal{J}_\phi(f) \quad (3)$$

Thus the phase process can be interpreted as additive noise for this case and produces hash sidelobes.

(B) In a CW the signal bandwidth can be very narrow because of the long integration times. In this case the spectrum of the phase

---

<sup>\*</sup>Note: Throughout the paper an impulse of unit area at  $(f = 0)$  is denoted  $\mu_o(f)$ .

process is wider than the signal spectrum ( $\Omega > \frac{1}{T}$ ) and the delay time is less than the pulse length ( $T_d < T$ ) therefore the spectrum of the received signal is

$$\mathcal{S}_R(f) = |\mathcal{S}_I(f)|^2 + 4\mathcal{S}_\phi(f) [1 - \cos 2\pi f T_d] \quad (4)$$

(C) If an IF crystal oscillator is used as the coherent reference in a pulsed radar, the spectrum of the phase process is narrower than the spectrum of the signal ( $\Omega < \frac{1}{T}$ ) and the delay is greater than a pulse length ( $T_d > T$ ). In this case the convolution in equation 1 must be evaluated. The results calculated numerically are a function of the spectrum of the phase process and sidelobe weighting. For  $\Omega T < .1$  there is almost no loss in resolution or achievable sidelobe level. For  $\Omega T > 10$  the results reduce to case A. For  $.1 < \Omega T < 10$  there is a loss in resolution where the sidelobe level is a linear function of  $\sqrt{\Omega T}$ .

The fourth relationship of delay, pulse length and phase bandwidth ( $T_d < T$ ,  $\Omega < \frac{1}{T}$ ) corresponds to a CW radar but is not likely to occur in practice because very narrow filters to limit the phase error bandwidth are not easily realized.

In all cases it is assumed that the RMS phase error is less than one radian. This assumption, which is valid for state-of-the-art coherent radars, makes the distortion sidelobes a linear function of the RMS phase error.

## SECTION II

### CALCULATION OF TRANSMIT SIGNAL SPECTRUM

Consider a pulsed transmit signal of the form

$$s_T(t) = \sqrt{\frac{2}{T}} e^{j\omega_0 t + j\phi(t)} \left[ \text{rect} \left( \frac{t}{T} \right) \right] \quad (5)$$

where

$$\text{rect} \left( \frac{t}{T} \right) = \begin{cases} 1 & \text{for } -\frac{T}{2} < t < \frac{T}{2} \\ 0 & \text{otherwise} \end{cases}$$

The relationship of the various signals is shown in Figure 1. Let  $\phi(t)$  be a zero-mean stationary random process specified by the following correlation function and spectral density.<sup>†</sup>

$$E \left[ \phi(t)^2 \right] = R_\phi(0) < 1 \text{ radian}^2 \quad (6)$$

$$R_\phi(\tau) = E \left[ \phi(t) \phi^*(t - \tau) \right] = \int_{-\infty}^{\infty} \mathcal{S}_\phi(f) e^{+j2\pi f\tau} df$$

The signal  $s_T(t)$  is a random process because it is a function of a random process. The pulsed nature of  $s_T(t)$  however makes it a nonstationary random process and, therefore, in a strict sense its power spectral density is not defined.

---

<sup>†</sup> In the numerical examples given in a later section, the approximation of small RMS phase error is shown to be valid for available equipment.



This difficulty is overcome<sup>†</sup> by defining another random process  $S_T(f)$  which is linearly related to the first by a Fourier transform

$$S_T(f) = \int_{-\infty}^{+\infty} s_T(t) e^{-j2\pi ft} dt \quad (7)$$

The expected value of  $S_T(f)$  is zero, although its variance is not.

The product of  $\Delta f$  and the variance of  $S_T(f)$

$$[\Delta f] E[|S_T(f)|^2]$$

is interpreted as the energy which would appear at the output of a narrow filter centered on  $f$  and  $\Delta f$  wide. Thus, the variance is interpreted as the power spectral density of  $s_T(t)$ . The power spectral density is therefore defined

$$\begin{aligned} \mathcal{S}_T(f) &= E[|S_T(f)|^2] \\ &= E \left[ \int_{-\infty}^{+\infty} s_T(t) e^{-j2\pi ft} dt \int_{-\infty}^{+\infty} s_T^*(\alpha) e^{+j2\pi f\alpha} d\alpha \right] \end{aligned} \quad (8)$$

$$\mathcal{S}_T(f) = \int_{-\infty}^{+\infty} \int_{-\infty}^{+\infty} R_S(t, \alpha) e^{-j2\pi f(t-\alpha)} dt d\alpha \quad (9)$$

where  $R_S(t, \alpha) = E[s_T(t) s_T^*(\alpha)]$

---

<sup>†</sup> A more rigorous analysis giving the same results is given in the Appendix.

The resolution and sidelobe level of the signal  $s_T(t)$  are determined from the square root of the power spectral density  $\mathcal{S}_T(f)$ .

A more general interpretation of  $\mathcal{S}_T(f)$  can be made if the transmit signal has a rectangular time envelope. For this class of signal, the function  $\mathcal{S}_T(f)$  is interpreted as the variance of the voltage at the output of a filter matched to  $s_T(t)$ . This interpretation which is proved in the Appendix is valid even if the received signal is weighted (e.g., Taylor sidelobe weighting). If  $s_T(t)$  is an arbitrary time limited signal, a more complicated expression for  $\mathcal{S}_T(f)$  is defined which is interpreted as the output of a matched filter.

The expression for  $\mathcal{S}_T(f)$  is evaluated by substituting the definition of  $s(t)$  into  $R_S(t, \alpha)$ .

$$R_S(t, \alpha) = E \left[ e^{j\phi(t)} \text{rect} \left( \frac{t}{T} \right) e^{-j\phi(\alpha)} \text{rect} \left( \frac{\alpha}{T} \right) \right] \cdot \frac{2}{T} \quad (10)$$

where the transmit center frequency,  $\omega_0$ , is assumed to be zero to normalize the calculation. This normalization is valid because complex notation has been used in the analysis. If the variance of the phase is small, it may be expanded in a few terms of a power series and an approximate expression for the correlation function may be found by keeping terms of second order:



$$R_S(t, \alpha) = E \left[ \left[ 1 + j\phi(t) - \frac{\phi(t)^2}{2} \right] \left[ 1 - j\phi(\alpha) - \frac{\phi(\alpha)^2}{2} \right] \right] \text{rect} \left( \frac{t}{T} \right) \text{rect} \left( \frac{\alpha}{T} \right) \cdot \frac{2}{T} \quad (11)$$

$$R_S(t, \alpha) = \frac{2}{T} \left[ 1 - R_\phi(0) + R_\phi(t-\alpha) \right] \text{rect} \left( \frac{t}{T} \right) \text{rect} \left( \frac{\alpha}{T} \right) \quad (12)$$

Equation 9 becomes

$$\mathcal{S}_T(f) = \int_{-T/2}^{+T/2} \int_{-T/2}^{+T/2} \frac{2}{T} \left[ 1 - R_\phi(0) + R_\phi(t-\alpha) \right] e^{-j\alpha\pi f(t-\alpha)} dt d\alpha \quad (13)$$

The integral in Equation 13 is more easily solved by rotation of coordinates. Define, therefore,

$$\tau = t - \alpha$$

$$\mu = t + \alpha$$

The rectfunction serves to limit the range of the integration; therefore, by suitably defining the limits of the integral, the multiplication by  $\text{rect} \left( \frac{t}{T} \right)$  can be implicitly stated. This gives

$$\begin{aligned} \mathcal{S}_T(f) &= \frac{2}{T} \int_{-T}^{+T} d\tau \int_{-T+\tau}^{+T-\tau} d\mu \left[ 1 - R_\phi(0) + R_\phi(\tau) \right] e^{-j2\pi f\tau} \\ \mathcal{S}_T(f) &= \int_{-T}^{+T} 4 \left[ 1 - R_\phi(0) + R_\phi(\tau) \right] \left[ 1 - \frac{|\tau|}{T} \right] e^{-j2\pi f\tau} d\tau \end{aligned} \quad (14)$$

Recognizing a multiplication in the  $\tau$  domain as a convolution in the  $f$  domain and taking the transform of  $R_s(\tau)$  the spectrum can be written by inspection\* as

$$\begin{aligned} \mathcal{S}_T(f) = & 2T[1-R_\phi(0)] \left[ \frac{\sin \pi fT}{\pi fT} \right]^2 \\ & + 2T \mathcal{S}_\phi(f) \otimes \left( \frac{\sin \pi fT}{\pi fT} \right)^2 \end{aligned} \quad (15)$$

If  $S_I(f)$  is the transform of the ideal signal  $s_I(t)$  (i.e., no phase corruption) and  $R_\phi(0)$  is much less than 1 radian<sup>2</sup>, Equation 15 can be written in the more general form

$$\mathcal{S}_T(f) = [\mu_o(f) + \mathcal{S}_\phi(f)] \otimes |S_I(f)|^2 \quad (16)$$

This general equation is proven in the Appendix for the case where  $s_I(t)$  is an uncoded sinusoidal pulse with a rectangular envelope.

---

\*The transform of a rect is  $\frac{\sin x}{x}$ , the transform of a triangle

(rect  $\otimes$  rect) is

$$\left( \frac{\sin x}{x} \right)^2$$

### SECTION III

#### EFFECT OF FINITE DELAY

Before any processing of the return signal, the RF output of the antenna is mixed down to an IF frequency (see Figure 1). The IF frequency is usually such a small percentage of the RF frequency ( $\sim 1\%$ ) that the IF frequency may be assumed to be zero without affecting the following calculations. In a coherent system, the local oscillator (L.O.) used to mix down is referenced in phase to the transmitted signals. Therefore, if the propagation delay is short enough, any phase errors on the received signal should be cancelled by the L.O. It is found that the finite range delay  $[T_d]$  changes the phase process  $[\phi(t)]$  to a phase difference process  $[\Delta\phi(t)]$  with the modulated power spectral density given by:

$$\Delta\phi(f) = 2 \phi(f) [1 - \cos 2\pi f T_d] \quad (17)$$

This assertion is shown below. The received signal, after mixing down to IF, is

$$r(t) = \text{rect} \left| \frac{t - T_d}{T} \right| e^{j(\omega_o + \omega_d)(t - T_d) + j\phi(t - T_d)} e^{-j\omega_o t - j\phi(t)} \quad (18)$$

$$r(t) = e^{-j\phi_o} e^{j\omega_d t} e^{j\Delta\phi(t)} \text{rect} \left| \frac{t - T_d}{T} \right| \quad (19)$$

where  $\Delta\phi(t) = \phi(t - T_d) - \phi(t)$

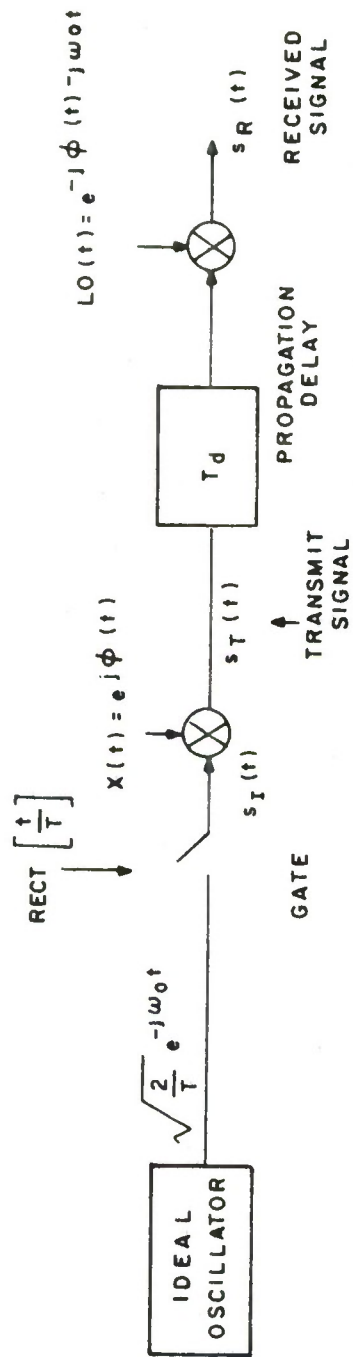


Figure 1. RELATIONSHIP OF RADAR SIGNALS

$$\phi_0 = (\omega_d + \omega_0) T_d$$

The phase  $\phi_0$  is not of interest and is ignored. Set the doppler frequency  $\omega_d$  and the center frequency  $\omega_0$  to zero for convenience. This is permissible because of the complex notation used throughout the paper.

The phase difference process is a stationary random process because it is a linear combination of stationary random processes. Thus, the problem reduces to the problem solved in the last section where now the phase difference spectral density  $\Delta\phi(f)$  is substituted for  $\phi(f)$  in Equation 16.

The spectral density of  $\Delta\phi(t)$  is found as follows:

$$\Delta\phi(f) = \int_{-\infty}^{\infty} R_{\Delta\phi}(\tau) e^{-j2\pi f\tau} d\tau \quad (20)$$

where

$$R_{\Delta\phi}(\tau) = E [\Delta\phi(t) \cdot \Delta\phi(t - \tau)]$$

Substituting the definition of  $\Delta\phi(t)$  into the above equation for the correlation function gives

---


$$R_{\Delta\phi}(\tau) = [\phi(t) - \phi(t - T_d)] [\phi^*(t - \tau) - \phi^*(t - \tau - T_d)] \quad (21)$$

$$R_{\Delta\phi}(\tau) = 2 R_{\phi}(\tau) - R_{\phi}(\tau + T_d) - R_{\phi}(\tau - T_d)$$

Using the Fourier theorem relating delays in one domain to linear phase in the other domain the spectral density is found:  $[R_{\phi}(\tau + T_d)$  transforms to  $\phi(f) e^{j2\pi f T_d}]$

$$\Delta\phi(f) = 2 \phi(f) [1 - \cos 2\pi f T_d] \quad (22)$$

Therefore, the received power spectrum is a modified version of Equation 16, namely

$$S_R(f) = |S_I(f)|^2 + 2[\phi(f)(1 - \cos 2\pi f T_d)] \times |S_I(f)|^2 \quad (23)$$

## SECTION IV

### APPLICATIONS AND NUMERICAL EXAMPLES

Applying the previous analysis to practical radar problems involves interpreting the expression for the received power spectral density given in Equation 23.

$$\mathcal{S}_R(f) = |S_I(f)|^2 + 2 \left[ \mathcal{S}_\phi(f) [1 - \cos 2\pi f T_d] \right] \otimes |S_I(f)|^2 \quad (24)$$

The spectral density is made up of two additive terms, the first is the power spectrum of the ideal signal  $|S_I(f)|^2$ , and the second is an error term involving the random phase spectrum. Because the second term has a convolution, it is not always easy to determine the effects of the phase errors by inspection. Fortunately, there are some limiting cases which correspond to practical radar situations for which the convolution is trivial. These cases are: (A) the bandwidth of the signal is narrow relative to  $\mathcal{S}_\phi(f)$  but broad relative to  $\cos(2\pi f T_d)$  or (B) the signal is very long in time so that  $S_I(f)$  appears as an impulse relative to  $\mathcal{S}_\phi(f) [1 - \cos 2\pi f T_d]$ . A third case (C) is non-trivial and requires a numerical evaluation of the convolution, because the bandwidth of  $S_I(f)$  and  $\mathcal{S}_\phi(f)$  may be approximately the same.

#### CASE A PULSED RADAR - MICROWAVE OSCILLATOR

Consider an X band pulsed radar with the rectangular pulse being generated by a microwave oscillator. Even a high Q cavity (say

$Q = 10^5$ ) will have a phase error bandwidth ( $\Omega$ ) of about 100 KHz. Assume that the pulse length ( $T$ ) is about one millisecond and the propagation delay ( $T_d$ ) is 5 milliseconds. Therefore, the following approximations are valid

$$\Omega > \frac{1}{T}$$

$$T < T_d$$

The power spectral density of the received signal is given by

$$S_R(f) = 2T \left[ \frac{\sin \pi f T}{\pi f T} \right]^2 + 4T S_\phi(f) [1 - \cos 2\pi f T_d] \left( \frac{\sin \pi f T}{\pi f T} \right)^2 \quad (25)$$

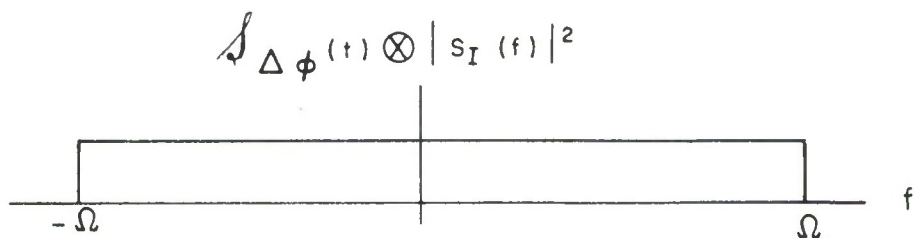
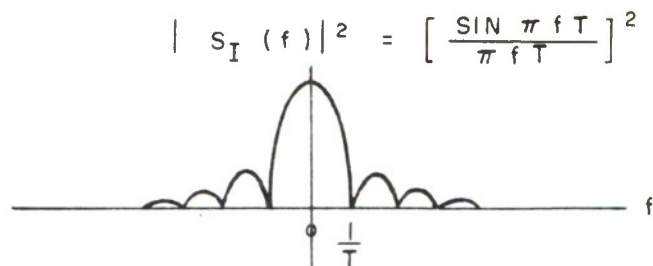
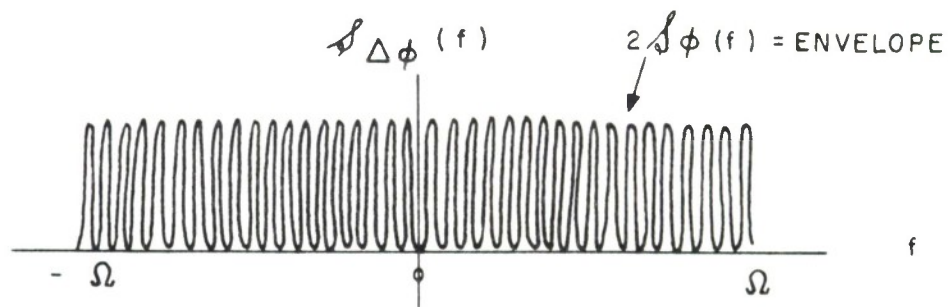
For the assumptions made the  $\left( \frac{\sin x}{x} \right)^2$  function looks like an impulse (of area  $\frac{1}{T}$ ) relative to the wide character of  $S_\phi(f)$  but is much wider than the period of the  $\cos 2\pi f T_d$  modulation. Therefore, the cosine term tends to average out. If  $T_d > 5T$  there are at least five cycles of the periodic function to be averaged and the approximation is good (see Figure 2). Thus, the receive power spectrum, plotted in Figure 2, is given by:

$$S_R(f) = 2T \left[ \frac{\sin \pi f T}{\pi f T} \right]^2 + 4S_\phi(f) \quad (26)$$

Let

$$S_\phi(f) = \frac{N_o}{2} \quad |f| < \Omega$$





DOPPLER RESOLUTION

1B-22,786

$$\frac{1}{T} \ll \Omega$$

$$T \ll T_d$$

Figure 2. SPECTRUM OF RECEIVED SIGNAL CASE A-WIDE BAND PHASE

then the RMS phase error is  $\overline{\phi^2} = R_\phi(0) = N_o \Omega$ . The signal-to-noise ratio (due to transmit phase errors only) is, therefore,

$$\begin{aligned} \left(\frac{S}{N}\right)^2 &= \frac{(\text{peak signal})^2}{\text{mean square noise}} \\ &= \frac{2T}{2N_o} = \frac{T\Omega}{\overline{\phi^2}} \end{aligned} \quad (27)$$

If  $T = 1$  millisecond,  $\Omega = 100$  Kc, and  $\sqrt{\overline{\phi^2}} = .1$  radian, the hash sidelobe level (which is the signal-to-noise ratio inverted) is

$$\text{RMS Sidelobe} \approx -40 \text{ db} \approx \left[\frac{S}{N}\right]^{-1} \quad (28)$$

The RMS sidelobe level (near the main lobe region) is proportional to the RMS phase error  $\left(\overline{\phi^2}\right)$  and inversely proportional to the square root of  $\Omega T$ .

#### CASE B CW RADAR

In a CW radar, the integration time (effective pulse length) is usually long relative to the propagation delay ( $T > T_d$ ). For the same reason the signal bandwidth is narrow relative to the phase process bandwidth regardless of the type of oscillator used. Even the best crystal oscillators have a phase error bandwidth of about 100 Hz. Thus, if the integration time is of the order of seconds, the following approximation is valid.

$$\Omega > \frac{1}{T}$$

Referring to Equation 24 the  $\left(\frac{\sin x}{x}\right)^2$  function looks like an impulse (of area  $1/T$ ) relative to the wide character of  $\mathcal{S}_\phi(f)$ . It also looks like an impulse relative to the  $(1 - \cos 2\pi f T_d)$  modulation, (see Figure 3). The cosine term does not average out. The spectrum of the receive signal, plotted in Figure 3, is given by

$$\mathcal{S}_R(f) = 2T \left( \frac{\sin \pi f T}{\pi f T} \right)^2 + 4 \mathcal{S}_\phi(f) (1 - \cos 2\pi f T_d) \quad (29)$$

This case corresponds to the calculation made by Raven<sup>[3]</sup>. For the sake of comparison, the same type of oscillator will be analyzed. A rather thorough discussion of oscillator stability may be found in an article by Cutler and Searle<sup>[6]</sup>. Based on their analysis a crystal oscillator may have the following characteristics:

Signal-to-noise ratio, $\frac{P_n}{P_s}$	87 db
$\frac{\Delta f}{f}$ for 1 sec	$1.4 \times 10^{-12}$
$\frac{\Delta f}{f}$ for 10 msec	$2 \times 10^{-10}$
phase bandwidth, $f_1$	100 Hz

The spectral density of the phase is approximately given by the following single-pole characteristic.\*

$$\mathcal{S}_\phi(f) = \frac{1}{2\pi f_1} N^2 \frac{P_n}{P_s} \frac{(f_1)^2}{(f_1)^2 + (f)^2} \quad (30)$$

\* The phase variance  $R_\phi$  for this oscillator (after frequency multiplication) is given by the area under  $\mathcal{S}_\phi(f)$  or approximately

$$N^2 \frac{P_n}{P_s} = .008 \text{ radian}^2.$$

This makes the approximation that  $R_\phi(0) < 1$  valid.

$$[1 - \cos 2\pi f T_d]$$

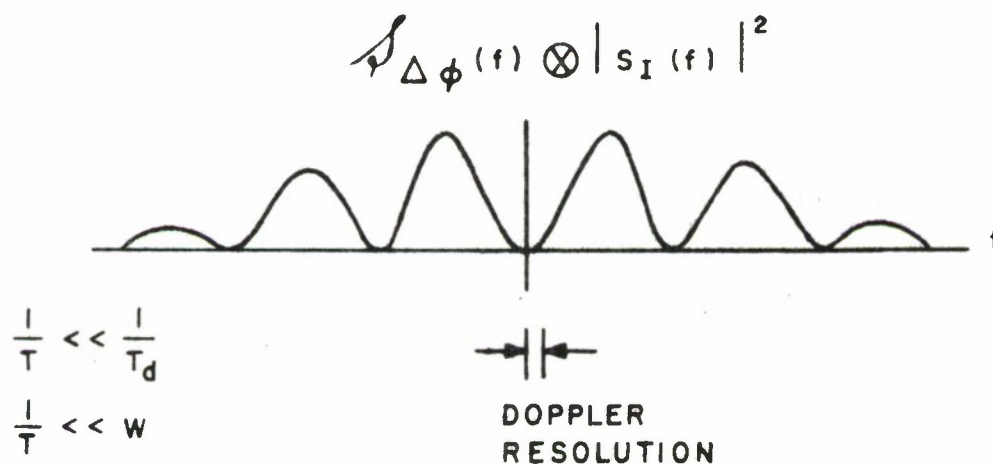
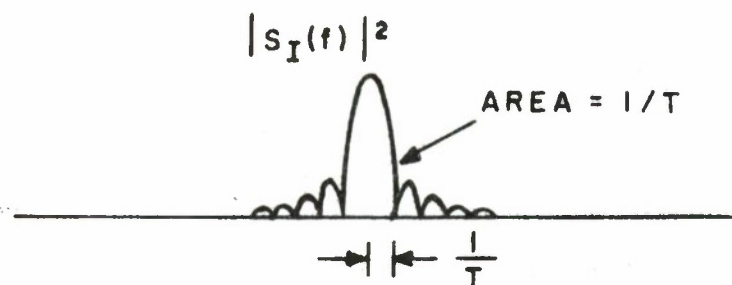
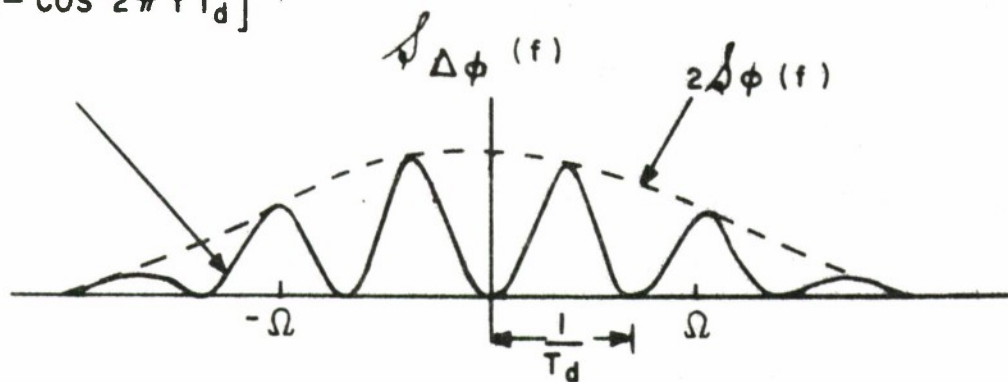


Figure 3. SPECTRUM OF RECEIVED SIGNAL CASE B - CW RADAR

The parameter  $N$  is the multiplication factor required to get the IF standard to the RF frequency. For the example let the transmit signal be at X band (10 GHz), therefore

$$N = \frac{10 \text{ GHz}}{5 \text{ MHz}} = 2000$$

Let the integration time be 1 second ( $T = 1$ ) and the range delay be 500  $\mu\text{sec}$ . This spectrum of the received signal is plotted in Figure 4.\* The envelope of the spectrum is shown in dotted lines  $\left(2\mathcal{S}_{\phi}(f)\right)$  while the spectrum itself  $2\mathcal{S}_{\phi}(f) (1 - \cos 2\pi f T_d)$  is shown in the solid line.

If the integration time were only 100 milliseconds then the hash sidelobe level would be 10 db higher.

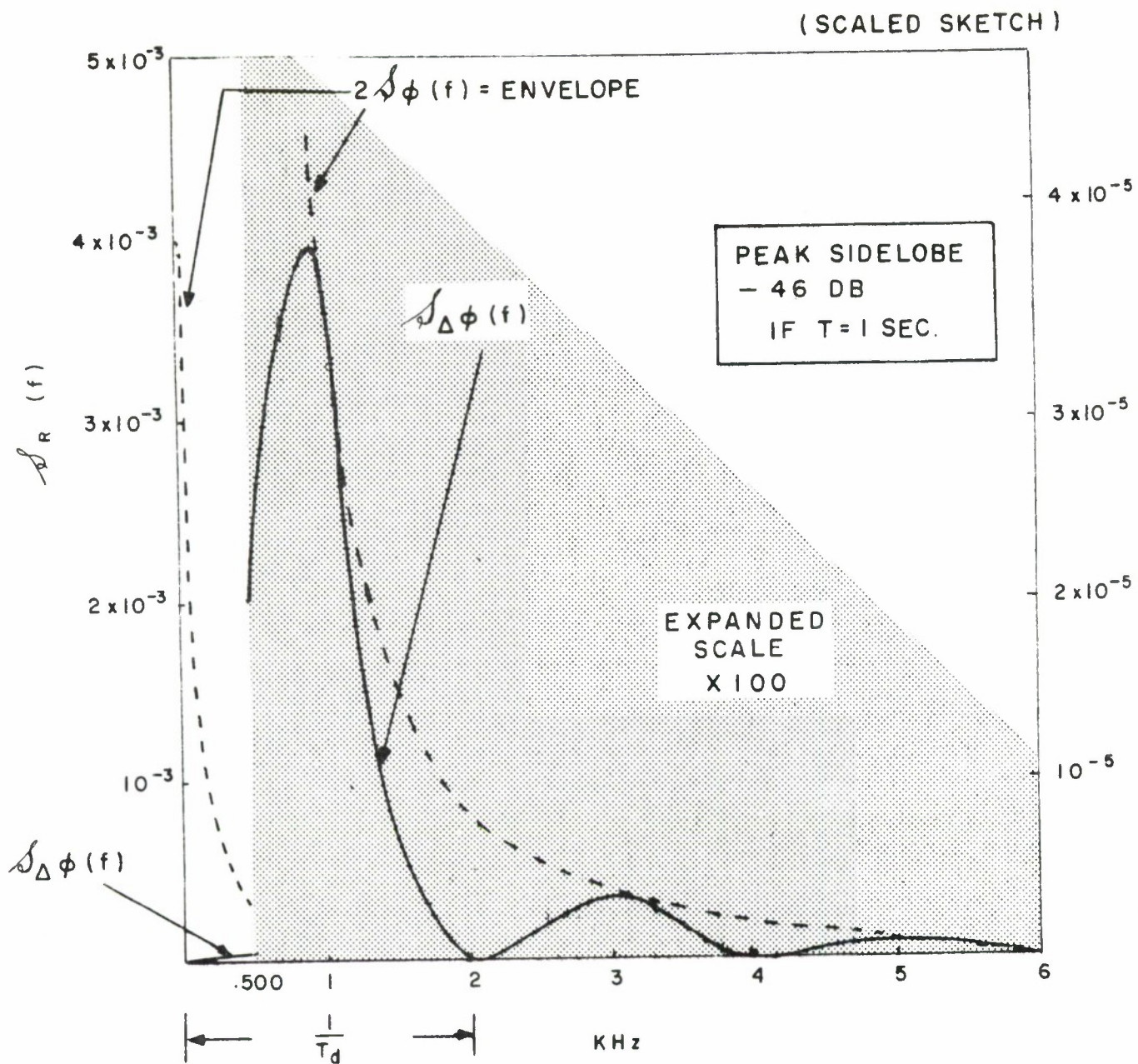
#### CASE C PULSED RADAR - CRYSTAL OSCILLATOR

In many radar situations the bandwidth of the phase process is not wide relative to the signal bandwidth  $\frac{1}{T}$ . Therefore, the convolution in Equation 24 is not easy to interpret. Only in the opposite limiting case where  $\Omega < \frac{1}{T}$  is the convolution again trivial.

If the phase spectral density ( $\mathcal{S}_{\phi}(f)$ ) is very narrow relative to the signal spectrum  $|S_I(f)|^2$  and the variance of the phase is small ( $R_{\phi}(0) < 1 \text{ radian}^2$ ) then the loss in resolution and sidelobe level is negligible.

---

\*Note. Figure 4 corresponds to Figure 7 in the Raven paper<sup>[3]</sup>. There is a difference only in the magnitude of the curve because the crystal oscillator described by Cutler & Searle<sup>[6]</sup> was used in the calculations made in this paper.



IB-22,785

Figure 4. RECEIVED SIGNAL POWER SPECTRUM - CW SIGNAL



In general this may not be a valid approximation, therefore the more general problem must be solved. Consider a pulsed radar using a crystal standard as its coherent reference which may have a 100 Hz noise bandwidth. If the pulse length is between one and ten milliseconds, then  $\Omega \approx \frac{1}{T}$ . The ratio of the phase process bandwidth to the signal bandwidth  $\frac{\Omega}{W} = \Omega T$  is a convenient measure to characterize the phase-signal relationship. Cases A and B correspond to  $\Omega T > 1$ , while the trivial case of C corresponds to  $\Omega T < 1$ . To describe the nature of the distortion for the general case of C ( $.1 < \Omega T < 10$ ) the following numerical analysis is required.

In a pulsed radar, the propagation delay is greater than the pulse length ( $T_d > T$ ). (For the calculations described below, the propagation delay is arbitrarily defined  $T_d = 5T$ .) The convolution was evaluated for values of  $T_d$  between  $2T$  and  $3T$  and between  $5T$  and  $6T$  in increments of  $.2T$ . In all cases, the variation in the sidelobe level is less than .3 db. Therefore for a pulsed radar with small RMS phase errors, the oscillator phase is essentially uncorrelated on transmit and receive.

A digital computer (SDS-930) was programmed to calculate and plot  $\mathcal{S}_R(f)$ . This function, as mentioned earlier and proven in the Appendix, can be interpreted as the variance of the voltage at the output of a filter matched to  $e^{j\omega_0 t} \text{rect}\left(\frac{t}{T}\right)$ . This interpretation is also valid if the received signal is weighted to reduce its sidelobes.

The function calculated is

$$\mathcal{J}_R(f) = |S_I(f)|^2 + 2 \mathcal{J}_\phi(f) (1 - \cos 2\pi f T_d) |S_I(f)|^2 \quad (31)$$

To include the effects of sidelobe weighting the ideal signal  $s_I(t)$  is multiplied by the function defined by Taylor weighting to achieve 30 db and 45 db sidelobes (see Klauder)<sup>[7]</sup>.

The spectral density of the phase is assumed to have the following one-pole low-pass characteristic:

$$\mathcal{J}_\phi(f) = \frac{2\Omega R_o}{(2\pi f)^2 + (\Omega)^2} \quad (32)$$

To provide a reference, the power spectrum of the undistorted signal ( $\sqrt{R_o} = 0$ ) is plotted in Fig. 5 for 30 db and 45 db Taylor weighting. In this figure, as in all the figures plotting  $\mathcal{J}_R(f)$ , the function is plotted in db (i.e. a log scale) and only the envelope of the sidelobes shown. That is, the peaks of the sidelobes are used to give data points and a smooth curve drawn between them. In almost all cases, the detailed sidelobe structure is uninteresting and tends to clutter a graph, especially one drawn on a log scale. On each graph, three curves are drawn, corresponding to  $\Omega T = 0.1, 1.0$ , and 10. The figure numbers, the degree of weighting and the RMS phase error used are given in the following table.



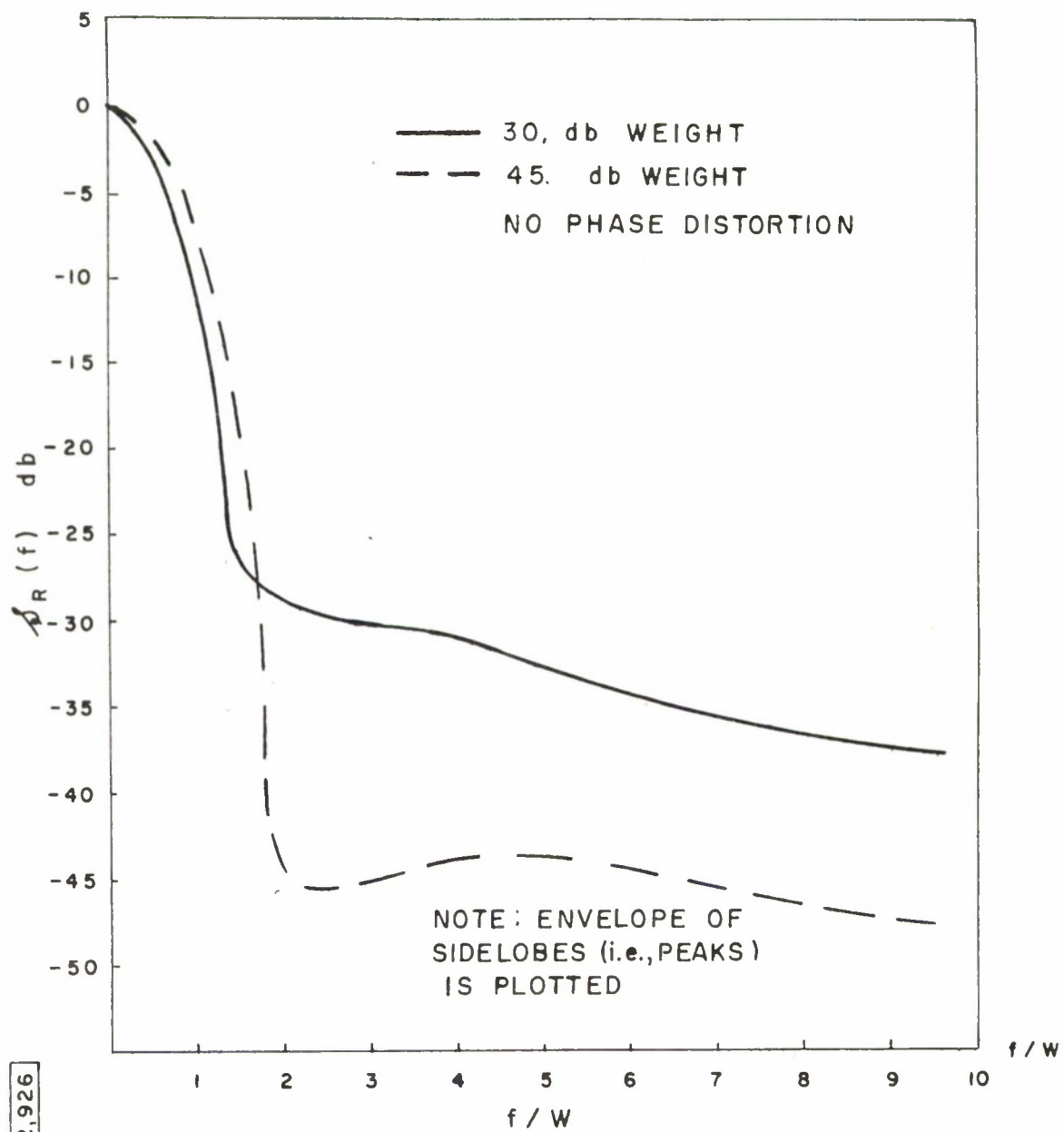


Figure 5. RECEIVED SIGNAL POWER SPECTRUM

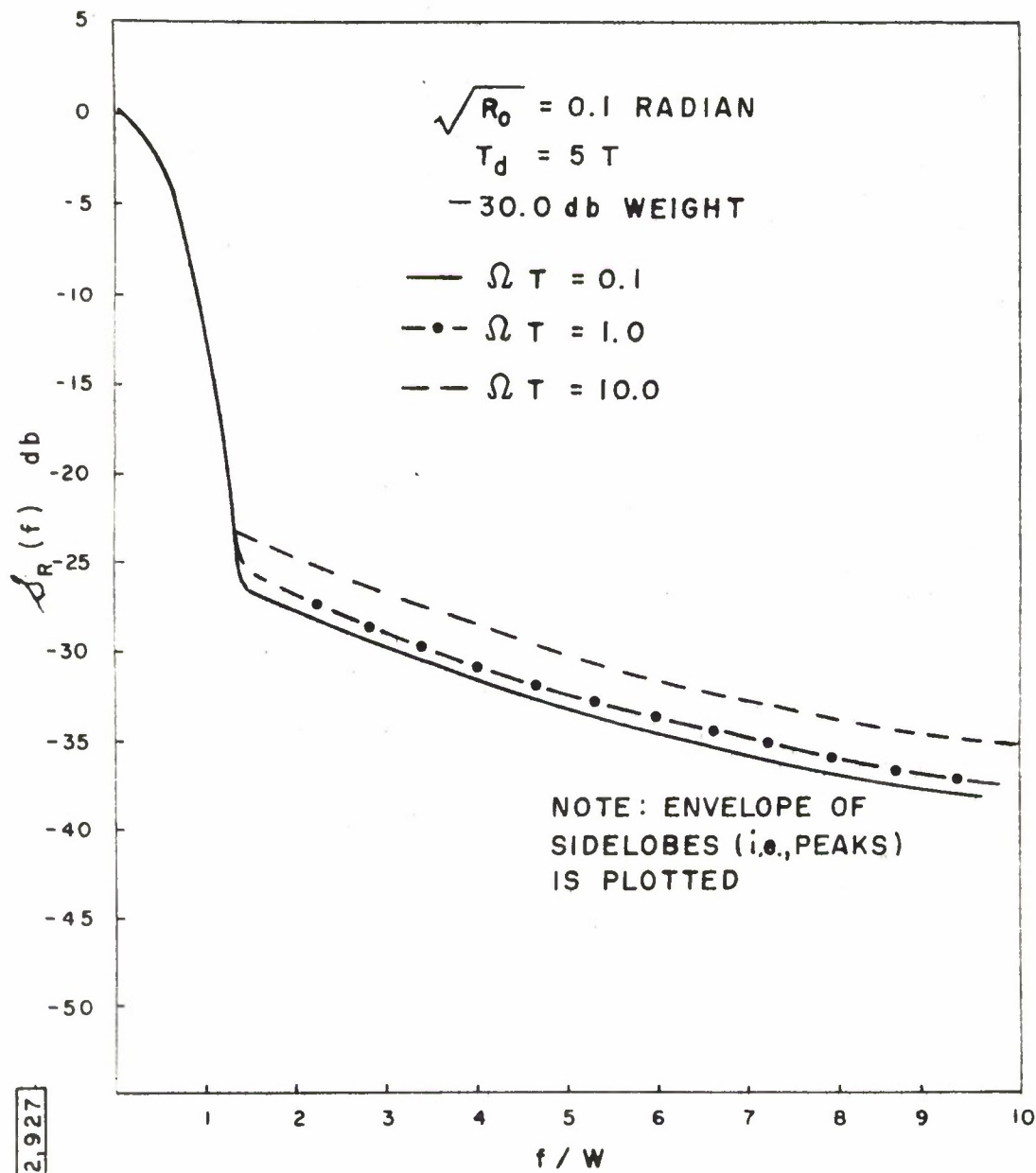
Table of Figures Plotting

$$\mathcal{J}_R(f)$$

Figure #	Taylor Weighting	RMS phase, $\sqrt{R_0}$
6	30	.1 radian ( $6^\circ$ )
7	30	.4 radian ( $24^\circ$ )
8	45	.1 radian
9	45	.4 radian

From these figures, it is apparent that the main lobe width is virtually unaffected by the phase distortion. The signal weighting tends to smear the curves so that structure of the curve is not strongly affected by  $\Omega T$ . The sidelobe level, however, is a strong function of  $\Omega T$ . To determine the dependence, the power spectral density is evaluated at an arbitrary value of  $f$ , removed from the main lobe region. (The value chosen was  $f = \frac{4.5}{T}$ ). The sidelobes vs  $\Omega T$  are plotted in Figure 10 for 45 db Taylor weighting and for  $\sqrt{R_0} = .4$  radians. In addition to the data given in Figure 9, the sidelobe level was evaluated at  $\Omega T = .01, .05, .5$ , and  $5.0$  to give a more comprehensive graph. Lack of computer storage capacity made calculations for  $\Omega T = 50, 100, 500$ , and  $1000$  inaccurate and unreliable.

Figure 10 is particularly enlightening. Computer calculations showed that for  $0.1 < \Omega T < 10$  the sidelobes grow proportional to  $\Omega T$ . For  $\Omega T < .01$  the sidelobe distortion is negligible. For  $\Omega T > 50$ , Equation 27 predicted the sidelobes would drop off as  $1/\sqrt{\Omega T}$ .



IA-22,927

Figure 6. RECEIVED SIGNAL POWER SPECTRUM

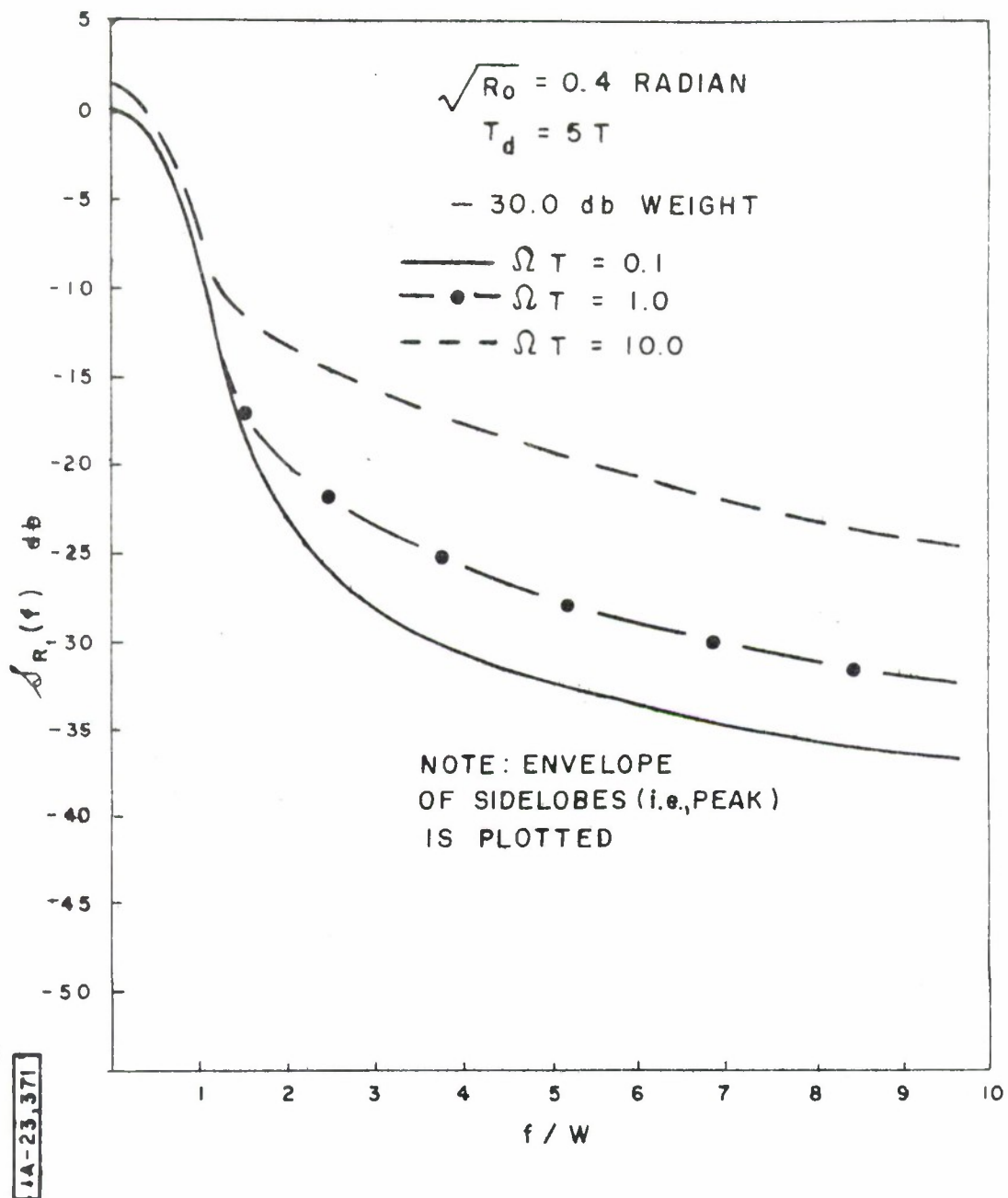


Figure 7. RECEIVED SIGNAL POWER SPECTRUM

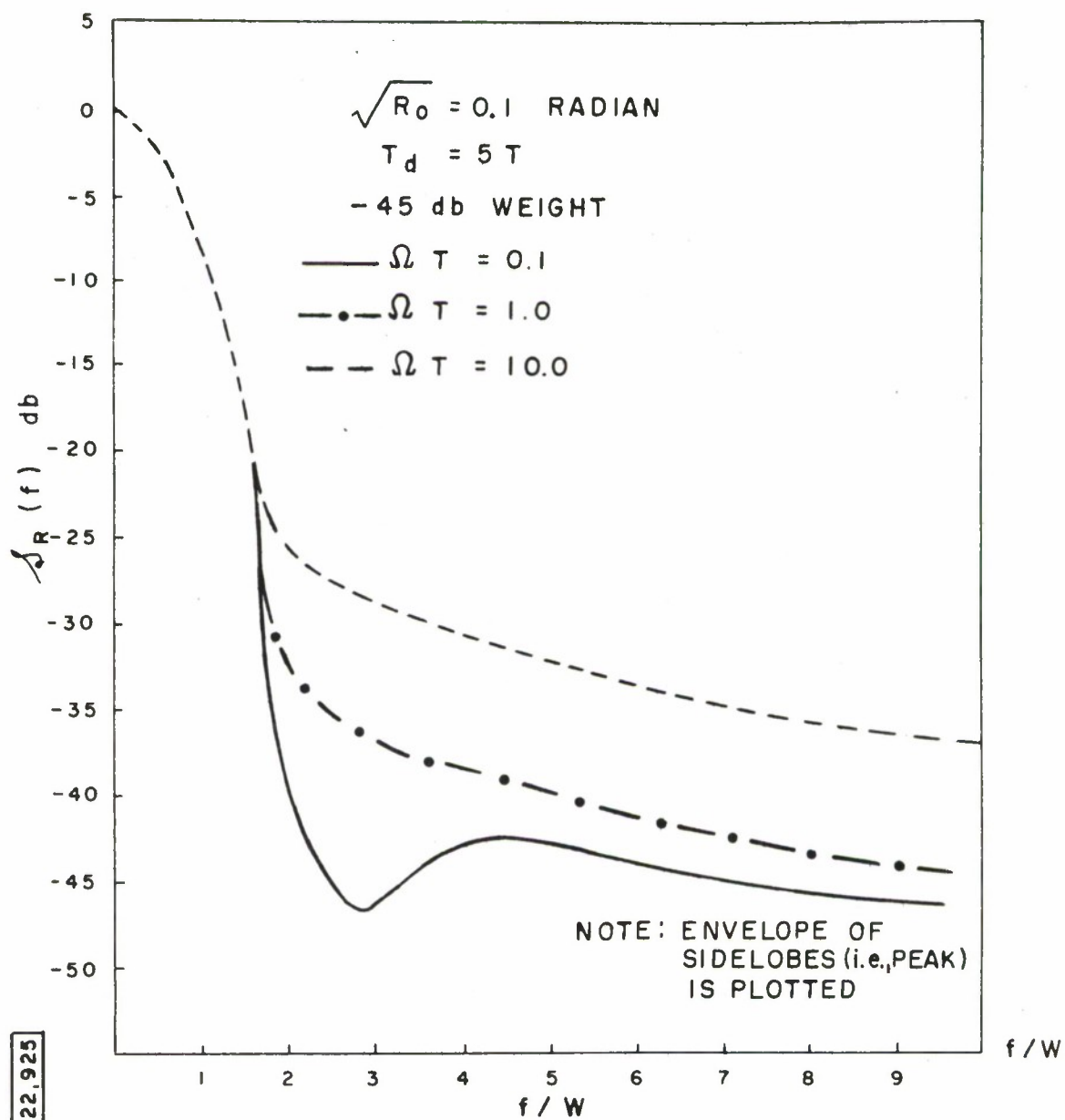
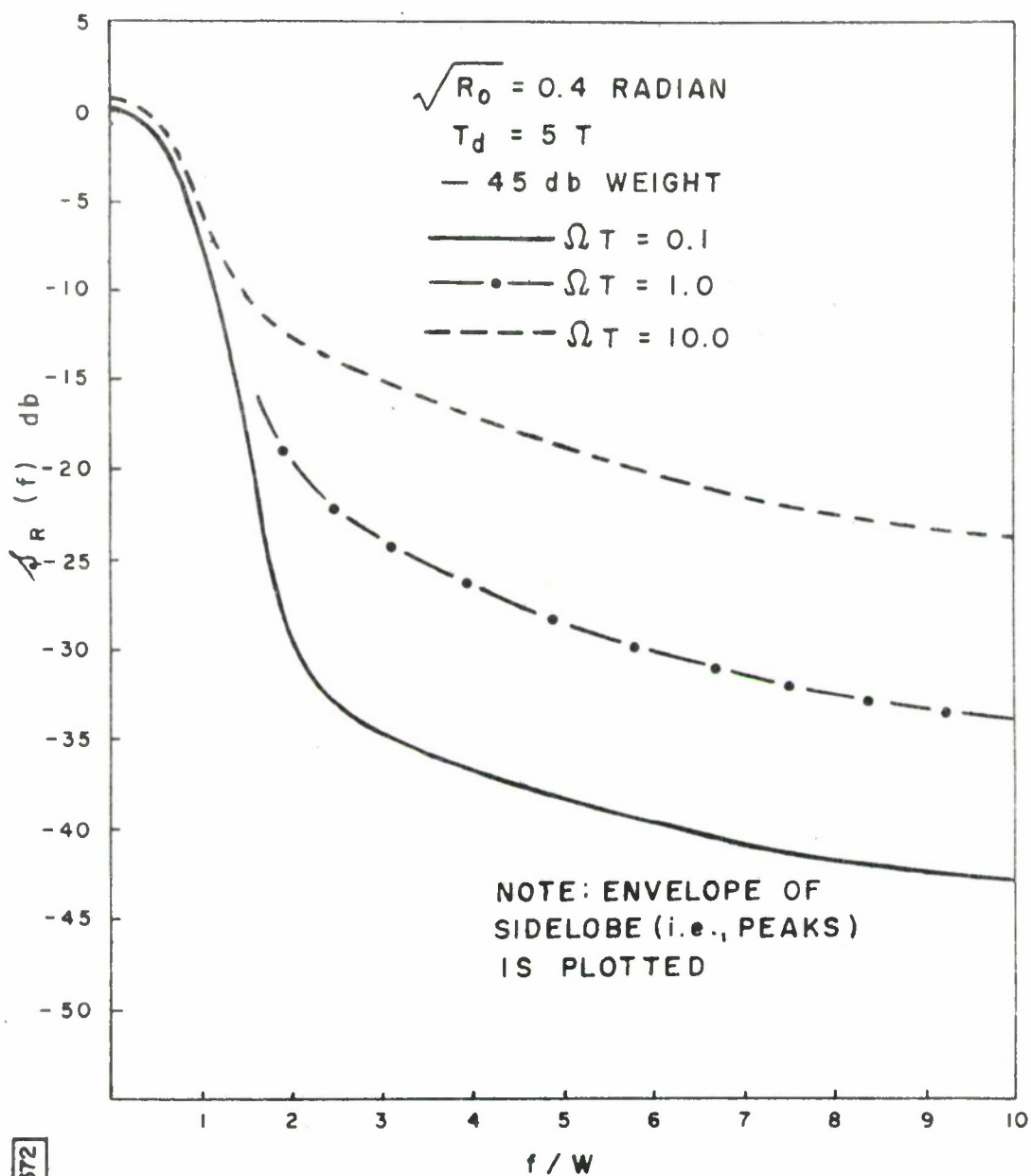


Figure 8. RECEIVED SIGNAL POWER SPECTRUM



1A-23,372

Figure 9. RECEIVED SIGNAL POWER SPECTRUM

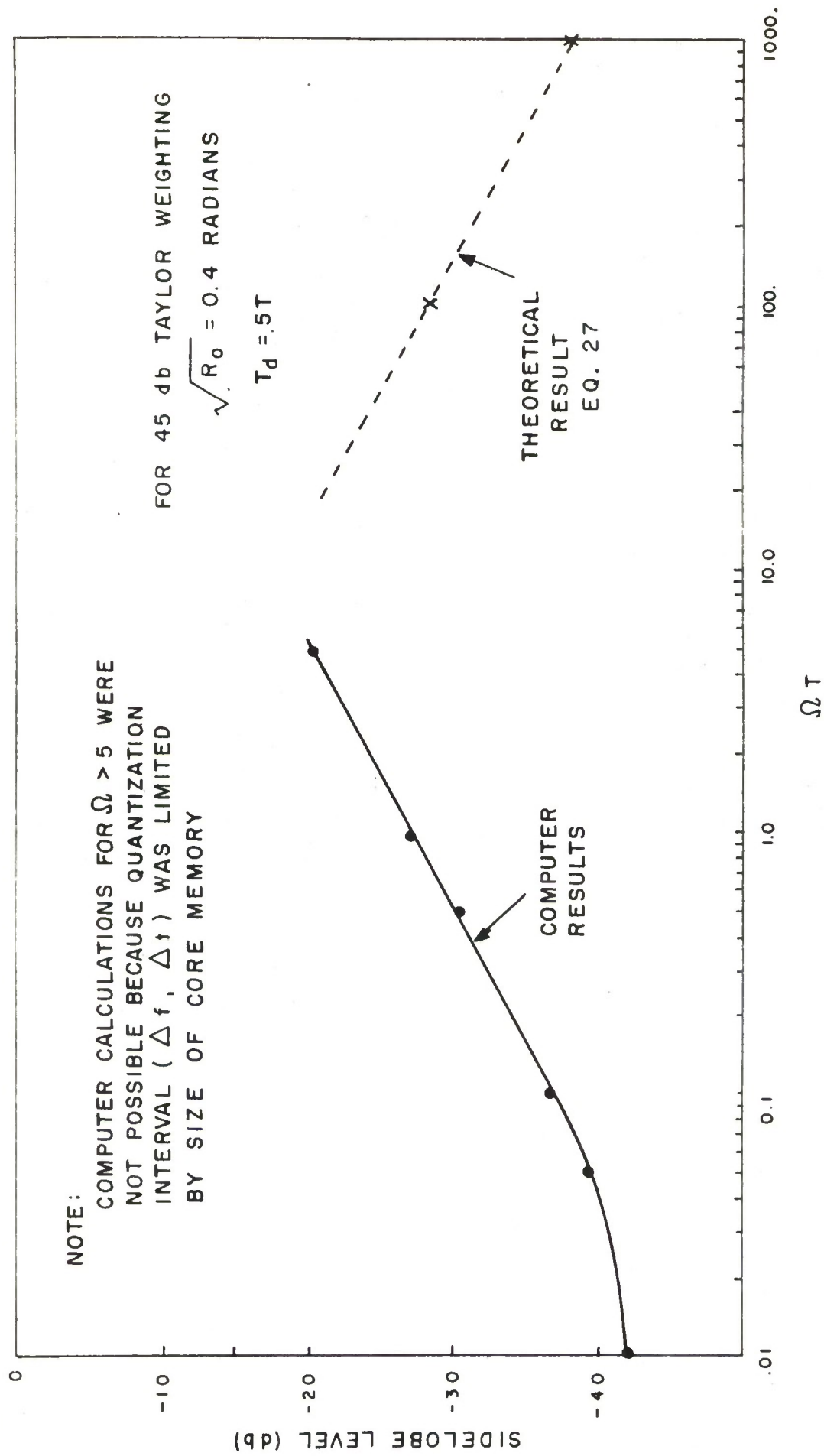


Figure 10. SIDELobe LEVEL  $\left[ \mathcal{S}_R \left( \frac{4.5}{T} \right) \right]$  VS  $\Omega T$

This curve is drawn in Figure 10 as a dashed line.\* The curve therefore consists of three almost straight line segments with slopes: 0,  $\Omega T$ , and  $1/\sqrt{\Omega T}$ . It is important to realize that the two break-points completely specify the sidelobe level and that these are a function of both the RMS phase error ( $\sqrt{R_o}$ ) and the degree of weighting. A complete specification of the dependence of the sidelobe level on  $\Omega T$  requires a four-dimensional plot. Instead of attempting to do this, it is hoped that the data given sufficiently illuminates the problem and that the equations derived allow one to calculate special cases should they arise.

---

\* Use of -45 db Taylor weighting will degrade the sidelobe level or signal-to-noise ratio by 2.68 db. The theoretical portion of Figure 10 is drawn without the effects of weighting included.



## SECTION V

### SUMMARY

The loss in resolution in terms of the increase in mainlobe width and the increase in sidelobe level is computed for radar signals corrupted by a stationary random phase process. By assuming that the RMS phase error is small, a relatively simple and easily interpretable analysis is possible.

A serious analytical difficulty arises in attempting to define a function from which the main lobe width and sidelobes could be calculated. The difficulty comes about because the statistics of the signal are not stationary; because of the pulsed nature of the signal, the signal statistics are time varying.

Two approaches are taken to solve the problem and both give the same solution for most signals of interest. The first approach treats the Fourier transform of the corrupted signal as a random process, because it is a linear function of a random process. The variance of this random process is interpreted as the variance of the voltage which would appear at the output of a very narrow filter if the corrupted signal were applied at its input. This approach is analytically the same as interpreting the beamwidth and sidelobe level of an antenna by calculating the expected power vs. angle.

The second approach given in the Appendix is more rigorous and is supported by detailed calculations. The corrupted signal is

applied to a filter matched to the uncorrupted signal but offset in frequency. The variance of the peak voltage at the output as a function of the offset frequency is calculated. Thus, the main lobe width and sidelobe level are calculated in a manner identical to actual practice. If the signal is a rectangular pulse, with or without sidelobe weighting, the result is the same as the first approach. If the signal is a general time limited signal, a more complicated expression for the matched filter output is derived.

In each approach, the required calculation requires convolving the phase spectral density with the power spectrum of the signal. The convolution is trivial in certain limiting cases where the bandwidth of the phase is much greater or much less than the bandwidth of the signal. A microwave oscillator has a very broad phase spectrum. Therefore, it tends to introduce error sidelobes while not affecting the main lobe width. A crystal oscillator, on the other hand, may have a very narrow phase spectrum, therefore the convolution must be evaluated. Numerical calculations revealed that again the main lobe width was not degraded but that hash sidelobes were introduced. The magnitude of the distortion sidelobes is very small for  $\Omega T < .01$  and is approximately a linear function of  $\sqrt{\Omega T}$  in the region  $.1 < \Omega T < 10$ . The function then reaches a maximum and decreases inversely with  $\sqrt{\Omega T}$  for  $\Omega T > 100$ . The sidelobes are also a linear function of the RMS phase error ( $\sqrt{R_o}$ ) for small values of that error.

The effect of a finite propagation is also considered. By using a coherent L.O. to mix down the received signal, most of the phase drift is cancelled if the propagation delay is short enough. Quantitatively, the delay introduces a  $(1 - \cos 2\pi f T_d)$  modulation on the phase spectrum. In the case of a CW radar, the modulation gives a sideband to the error sidelobes, while for a microwave oscillator (pulsed radar) the cosine modulation term averages out. In the more general case, the propagation delay must be included in the calculations. For  $f > 5/T_d$ , a common pulsed radar situation, the calculations indicate that the correlation between the transmit and receive phase errors may be ignored. In those cases where the phase process has a very narrow bandwidth and the transmit and receive phases are correlated, the product  $\Omega T$  is so small that the distortion is negligible.

## APPENDIX

### CALCULATION OF SPECTRA OF PULSED RANDOM PROCESS

The analysis presented in this appendix gives a more mathematical derivation of Equation 16 of the text which is an expression for the spectrum of a sinusoidal pulsed signal corrupted by a zero-mean stationary random phase. The approach of this analysis was first reported by Kramer in a private communication.

Assume an ideal uncorrupted signal  $s_I(t)$  of the form (see Figure 1 for graphical signal relationships)

$$s_I(t) = \sqrt{\frac{2}{T}} e^{j2\pi f_o t} \text{rect} \left( \frac{t}{T} \right) \quad (33)$$

The ideal signal is corrupted by a multiplicative distortion  $x(t)$ , where

$$x(t) = e^{j\phi(t)} \quad (34)$$

and  $\phi(t)$  is a stationary random process. The resultant corrupted signal is identified as a transmitted radar signal  $s_T(t)$  and is

$$s_T(t) = s_I(t) x(t) \quad (35)$$

If  $S_I(f)$  is the frequency function of  $s_I(t)$  and  $\mathcal{S}_x(f)$  the power spectral density of  $x(t)$  then a suitably defined power spectral

density of  $s_T(t)$  will be shown to be

$$\mathcal{S}_T(f) = |s_I(f)|^2 \otimes \mathcal{S}_\phi(f) \quad (36)$$

If the variance of  $\phi(t)$  is small, i.e.,

$$R_\phi(0) = \overline{|\phi(t)|^2} \ll 1 \text{ radian}$$

then the suitably defined spectral density of  $s_T(t)$  is (Equation 16 of the text)

$$\mathcal{S}_T(f) = [\mu_\phi(f) + \mathcal{S}_\phi(f)] \otimes |s_I(f)|^2 \quad (37)$$

The power spectral density of  $s_T(t)$  is not rigorously defined because (1) the signal is not a stationary random process, and (2) the power in a narrow band  $\Delta f$  approaches zero as  $\Delta f$  approaches zero, (unlike the power spectral density of a stationary process). This difficulty is overcome by two different analyses which reach the same conclusion. The signal  $s_T(t)$  is passed through a filter with impulse response  $h(\tau)$ . If the filter is assumed to be very narrow in frequency at  $f_0$  the variance of its output can be interpreted as a measure of the spectral content of its input. On the other hand, if the filter is matched to the uncorrupted signal, except for a frequency offset  $f_d$ ,

$$h(\tau) = s_I(T - \tau) e^{j2\pi f_d \tau} \quad (38)$$

then the variance of its output  $\mathcal{S}_T(f_d)$  at  $t = 0$  is a function of the frequency offset of the filter  $(f_d)$ . This function is also interpreted as the spectral content of  $S_T(f)$ . Because matched filtering is used in practice, the system resolution and sidelobe capability is directly measured by  $\mathcal{S}_T(f_d)$ . The following detailed analysis supports these assertions. In addition, the equations are derived for the matched filter output for the case where  $s_I(t)$  is any time-limited signal.

The output of the filter  $y(t)$  is defined by the following convolution

$$y(t) = \int_{-\infty}^{\infty} h(t - \tau) s_I(\tau) d\tau \quad (39)$$

The mean square voltage at the output is given by

$$\begin{aligned} E[|y(t)|^2] &= \overline{y(t) y^*(t)} \\ &= \int_{-\infty}^{\infty} \int_{-\infty}^{\infty} h(t - \tau) h^*(t - \alpha) s_I(\tau) s_I^*(\alpha) \overline{x(\tau) x^*(\alpha)} d\tau d\alpha \end{aligned} \quad (40)$$

The transforms of the filter and correlation function are defined as follows:

$$\begin{aligned} h(t - \tau) &= \int_{-\infty}^{\infty} H(\nu_1) e^{+j2\pi\nu_1(t-\tau)} d\nu_1 \\ h^*(t - \alpha) &= \int_{-\infty}^{\infty} H^*(-\nu_2) e^{+j2\pi\nu_2(t-\alpha)} d\nu_2 \end{aligned} \quad (41)$$

$$s_I(\tau) = \int s_I(v_3) e^{+j2\pi v_3(\tau)} dv_3$$

$$s_I^*(\alpha) = \int s_I^*(-v_4) e^{+j2\pi v_4\alpha} dv_4$$

$$\overline{x(\tau) x^*(\alpha)} = R_x(\tau - \alpha) = \int_{-\infty}^{\infty} \mathcal{S}_x(v_5) e^{+j2\pi v_5(t-\alpha)} dv_5$$

Substituting these definitions for the transforms into Equation 40 gives the following sevenfold integral.

$$\begin{aligned} \overline{y(t) y^*(t)} &= \int d\tau \int d\alpha \int dv_1 \int dv_2 \int dv_3 \int dv_4 \int dv_5 H(v_1) H^*(-v_2) \cdot \\ &\quad s_I(v_3) s_I^*(-v_4) \mathcal{S}_x(v_5) e^{+j2\pi v_1(t-\tau)} e^{+j2\pi v_2(t-\alpha)} \cdot \\ &\quad e^{+j2\pi v_3\tau} e^{+j2\pi v_4\alpha} e^{+j2\pi v_5(t-\alpha)} \end{aligned} \quad (42)$$

Changing the order of the integration, the integrals over  $\tau$  and  $\alpha$  become

$$\int_{-\infty}^{\infty} e^{-j2\pi(v_1-v_3-v_5)\tau} d\tau \cdot \int_{-\infty}^{\infty} e^{-j2\pi(+v_2-v_4+v_5)\alpha} d\alpha \quad (43)$$

$$= \mu_o(v_1-v_3-v_5) \mu_o(v_2-v_4+v_5) \quad (44)$$

The integration over  $v_3$  and  $v_4$  are then trivial and yield

$$\overline{y(t) y^*(t)} = \iiint d\nu_1 d\nu_2 d\nu_5 H(\nu_1) H^*(-\nu_2) S_I(\nu_1 - \nu_5) S_I^*(-\nu_5 - \nu_2) \mathcal{S}_x(\nu_5) \cdot e^{j2\pi\nu_1 t} e^{j2\pi\nu_2 t} \quad (45)$$

Now let the filter characteristic be very narrow, centered on  $f_d$  and with very large gain:

$$H(\nu_1) = \mu_0(\nu_1 - 2\pi f_d)$$

$$H(-\nu_2) = \mu_0(-\nu_2 - 2\pi f_d) \quad (46)$$

The mean square voltage per cycle at  $f_d$  is independent of time, is only a function of  $f_d$ , and is interpreted as the spectral density of  $s(t)$ ,  $\left[ \mathcal{S}_T(f_d) \right]$ .

$$\mathcal{S}_T(f_d) = \overline{y(t) y^*(t)} = \int S_I(f_d - \nu_5) S_I^*(f_d - \nu_5) \mathcal{S}_x(\nu_5) d\nu_5 \quad (47)$$

$$\mathcal{S}_T(f_d) = |S_I(f)|^2 \otimes \mathcal{S}_x(f) \quad (48)$$

If the phase is small the corrupting signal is

$$x(t) = e^{j\phi(t)} \approx 1 + j\phi(t) - \frac{\phi(t)^2}{2} \quad (49)$$



The correlation function can be approximated by

$$R_x(\tau) = \overline{x(t) x^*(t-\tau)} \approx 1 + R_\phi(\tau) \quad (50)$$

The spectral density is, therefore, given by

$$S_x(f) \approx \mu_o(f) + S_\phi(f) \quad (51)$$

Substitution into Equation 13 gives the desired result

$$S_T(f_d) = \left[ \mu_o(f) + S_\phi(f) \right] \otimes |S_I(f)|^2 \quad (52)$$

Rather than interpreting  $S_T(f_d)$  as the transmit power spectral density, as was just proven, it is sometimes possible to interpret  $S_T(f_d)$  as the variance of the voltage at the peak output of a filter matched to the transmit signal offset by  $(f_d)$ . This interpretation is possible when the transmit signal has a rectangular envelope  $\left( \text{rect } \frac{t}{T} \right)$  and holds whether the receive signal is weighted or unweighted. For a general time-limited signal, a more complicated expression defines the variance of the voltage at the matched filter output. These assertions are now proven.

The variance of the voltage output of an arbitrary filter is given by Equation 45 :

$$\overline{y(t) y^*(t)} = \iiint H(\nu_1) H^*(-\nu_2) S_I(\nu_1 - \nu_5) S_I^*(-\nu_2 - \nu_5) \mathcal{L}_x(\nu_5) e^{j2\pi(\nu_1 + \nu_2)t} d\nu_1 d\nu_2 d\nu_5 \quad (53)$$

Assume that the received signal is unweighted and has the form

$$s_I(t) = \sqrt{\frac{2}{T}} e^{j2\pi f_o t} \text{rect}\left(\frac{t}{T}\right) \quad (54)$$

Its transform is (assuming  $f_o = 0$  for analytical convenience)

$$S_I(f) = \frac{\sin \pi f T}{\pi f T} \quad (55)$$

Let the arbitrary filter,  $H(f)$  be matched to  $s_I(t)$  but offset by  $f_d$

$$H(f) = S_I^*(f - f_d) \quad (56)$$

Equation 53, evaluated at the peak of the matched filter output ( $t = 0$ ) becomes

$$\begin{aligned} \overline{y(0) y^*(0)} = & + \int d\nu_5 \mathcal{L}_x(\nu_5) \int \frac{\sin \pi(\nu_1 - f_d)T}{\pi(\nu_1 - f_d)T} \frac{\sin \pi(\nu_1 - \nu_5)T}{\pi(\nu_1 - \nu_5)T} d\nu_1 \cdot \\ & \int \frac{\sin \pi(\nu_2' - f_d)T}{\pi(\nu_2' - f_d)T} \frac{\sin \pi(\nu_2' - \nu_5)T}{\pi(\nu_2' - \nu_5)T} d\nu_2' \end{aligned} \quad (57)$$

where  $\nu_2' = -\nu_2$

Because of the following general relationship, this equation can be reduced:

$$\int \frac{\sin(x-x_0)}{(x-x_0)} \frac{\sin x}{x} dx = \frac{\sin x_0}{x_0} \quad (58)$$

$$\begin{aligned} \overline{|y(t)|^2} &= \int \mathcal{L}_x(\nu_5) \left[ \frac{\sin \pi(f_d - \nu_5)T}{\pi(f_d - \nu_5)T} \right]^2 d\nu_5 \\ &= \int \mathcal{L}_x(\nu_5) |s_I(\Delta\omega - \nu_5)|^2 d\nu_5 \end{aligned} \quad (59)$$

Equation 59 is the definition of a convolution and is interpreted as the variance of the output voltage of a filter matched to  $s_I(t)$  and offset by  $f_d$ .

$$\mathcal{L}_T(f_d) = \mathcal{L}_x(f) \otimes |s_I(f)|^2 \quad (60)$$

For weighted signals the analysis is modified slightly. Let the received weighted signal and its transform be

$$\begin{aligned} s_{wT}(t) &= s_T(t) w(t) \\ s_{wT}(f) &= \sum_{i=-\infty}^{\infty} w_i s_T(f - \frac{i}{T}) \end{aligned} \quad (61)$$

For practical applications, the above sum includes only a few terms [for example,  $1 + \cos \frac{2\pi t}{T}$  has coefficients  $w_{-1} = w_{+1} = \frac{1}{2}$ ,  $w_0 = 1$ , all other weights are zero].

The filter, however, is still matched to the unweighted signal. The equation for the variance of the peak matched-filter output is

$$\overline{y(0) y(0)^*} = + \int dv_5 \mathcal{S}_x(v_5) \int \Sigma w_i \cdot \frac{\sin \pi(v_1 - f_d)T}{\pi(v_1 - f_d)T} \frac{\sin \pi(v_1 - v_5 - \frac{i}{T})T}{\pi(v_1 - v_5 - \frac{i}{T})T} dv_i$$

$$\int \Sigma w_j \frac{\sin \pi(v_2' - f_d)T}{\pi(v_2' - f_d)T} \frac{\sin \pi(v_2' - v_5 - \frac{i}{T})T}{\pi(v_2' - v_5 - \frac{i}{T})T} dv_2' \quad (62)$$

This reduces to the same equation as before:

$$\overline{|y(0)|^2} = \int dv_5 \mathcal{S}_x(v_5) \left[ \Sigma w_i \frac{\sin \pi(f_d - v_5 - \frac{i}{T})T}{\pi(f_d - v_5 - \frac{i}{T})T} \right]^2 \quad (63)$$

$$= \int \mathcal{S}_x(v_5) |s_I(f_d - v_5)|^2 \quad (64)$$

The general case follows the same pattern. For any time-limited signal it is possible to write the transmit signal in the form

$$s_T(f) = \sum \lambda_i \frac{\sin \pi(f - \frac{i}{T})T}{\pi(f - \frac{i}{T})T} \quad (65)$$

The filter  $H(f)$  is matched to this signal, therefore,

$$H(f) = S_T^*(f - f_d) = \sum \lambda_i^* \frac{\sin \pi(f - \Delta f - \frac{i}{T}) T}{\pi(f - \Delta f - \frac{i}{T}) T} \quad (66)$$

The expression for the output variance is found by the same procedure, and gives

$$\overline{|y(0)|^2} = \int dv_5 \mathcal{S}_x(v_5) \sum \sum \lambda_i \lambda_j^* \frac{\sin \pi(f_d - \frac{i-j}{T} - v_5) T}{\pi(f_d - \frac{i-j}{T} - v_5) T} \quad (67)$$

This can be expressed as

$$\mathcal{S}_T(f_d) = \mathcal{S}_x(f) \otimes |U(f)|^2 \quad (68)$$

where

$$U(f) = \sum \sum \lambda_i \lambda_j^* \frac{\sin \pi(f - \frac{i-j}{T}) T}{\pi(f - \frac{i-j}{T}) T}$$

Equation 68 expresses the general result of the Appendix. Using numerical analysis techniques, it is possible to easily determine the loss in resolution and sidelobe level for any time limited signal.

If numerical techniques are used, it would also be possible to calculate the power density of  $x(t)$ , namely  $\mathcal{S}_x(f)$ , without assuming a small phase variance. Therefore, it is possible to calculate in a straightforward manner the system degradation due to

random phase errors for the general problem without making narrowing assumptions even though the final equation appears complicated.

#### REFERENCES

1. J. T. Lynch. "A Straightforward, General Analysis of Signal Distortion with Applications to Wideband Ionospheric Dispersion," ESD-TR-67-623, The MITRE Corporation, Bedford, Mass.
2. Proceedings of the IEEE, Frequency Stability Issue, Vol. 54, No. 2, February 1966.
3. R. S. Raven, Proceedings of the IEEE, Frequency Stability Issue, Vol. 54, No. 2, February 1966, pp. 237-243.
4. John Ruze, Ph.D. Thesis, 1952, MIT Research Laboratory of Electronics, Technical Report No. 248, October 30, 1952.
5. Jean Develet, "The Influence of Random Phase Errors on the Angular Resolution of Synthetic Aperture Radar Systems," Aerospace Corp., Report No. TDR-169(3250-43)TN-4, 20 June 1963.
6. L. S. Cutler and C. L. Searle. Proceedings of the IEEE, Frequency Stability Issue, Vol. 54, No. 2, February 1966, pp. 136-154.
7. J. R. Klauder et al. Bell Systems Technical Journal, Vol. XXXIX, No. 4, July 1960, pp. 745-808.

### BIBLIOGRAPHY

- Bracewell, R. N. "Tolerance Theory of Large Antennas," IRE Trans. on Antennas and Propagation, January, 1961.
- Brown, W. M. and C. J. Palermo "Effects of Phase Errors on the Ambiguity Function," IEEE Int. Conv. Record, VII, Part 4, 1963.
- Brown, W. M. and C. J. Palermo "Effects of Phase Errors on Resolution," IEEE Transactions on Military Electronics, July-October 1965.
- Brown, W. M. and C. J. Palermo "System Performance in the Presence of Stochastic Delays," Radar Laboratory, Inst. of Sci. and Tech., University of Michigan.
- Crimmins, T. R. and Harger, R. O., The Effect of Phase Errors on Weighted Spectra, IEEE Transactions on Military Electronics, July-October 1965, p 298-299.
- Cutler, L. S. and Searle, C. L., Proceedings of the IEEE, Frequency Stability Issue, Vol. 54, No. 2, February 1966, pp.136-154.
- Develet, Jean, "The Influence of Random Phase Errors on the Angular Resolution of Synthetic Aperture Radar Systems," Aerospace Corp., Report No. TDR-169(3250-43)TN-4, 20 June, 1963.
- Edson, W. A. "Noise in Oscillators," Proceedings of the IRE, August 1960.
- Elliott, Robert S. "Mechanical and Electrical Tolerances for Two-Dimensional Scanning Antenna Arrays," IRE Trans. on Antennas and Propagation, January 1958
- Klauder, J. R., et al, Bell Systems Technical Journal, Vol. XXXIX, No. 4, July 1960, pp. 745-808.
- Kurtz, L. A. and R. S. Elliott "Systematic Errors Caused by the Scanning of Antenna Arrays: Phase Shifters in the Branch Lines," IRE Trans. on Antennas and Propagation, October 1956, p. 619-627.
- Leeson, D. B. and Johnson, G. F., Short-Term Stability for a Doppler Radar: Requirements, Measurements, and Techniques, p 244-248.
- Leichter, M. "Beam Pointing Errors on Long Line Sources" IRE Trans.



on Antennas and Propagation, May 1960, p 268-275.

Lynch, J. T., "A Straightforward, General Analysis of Signal Distortion with Applications to Wideband Ionospheric Dispersion," ESD-TR-67-623, The MITRE Corporation, Bedford, Mass.

Raven, R. S. Proceedings of the IEEE, Frequency Stability Issue, Vol. 54, No. 2, February 1966, pp. 237-243.

Ruze, John, Ph.D. Thesis, 1952, MIT Research Laboratory of Electronics, Technical Report No. 248, October 30, 1952.

Sydnor, R. and Caldwell, J. J. and Rose, B. E., Frequency Stability Requirements for Space Communications and Tracking Systems, p231-236, Proceedings of the IEEE, February, 1966.

## DOCUMENT CONTROL DATA - R &amp; D

(Security classification of title, body of abstract and indexing annotation must be entered when the overall report is classified)

1. ORIGINATING ACTIVITY (Corporate author) <b>The MITRE Corporation Bedford, Massachusetts</b>		2a. REPORT SECURITY CLASSIFICATION <b>UNCLASSIFIED</b>	
		2b. GROUP <b>N/A</b>	
3. REPORT TITLE <b>EFFECT OF RADAR SYSTEM INCOHERENCE ON ACHIEVABLE MAINLOBE WIDTHS AND SIDELobe LEVELS</b>			
4. DESCRIPTIVE NOTES (Type of report and inclusive dates) <b>N/A</b>			
5. AUTHOR(S) (First name, middle initial, last name) <b>John T. Lynch</b>			
6. REPORT DATE <b>February 1968</b>		7a. TOTAL NO. OF PAGES <b>55</b>	7b. NO. OF REFS <b>17</b>
8a. CONTRACT OR GRANT NO. <b>AF 19(628)-5165</b>		9a. ORIGINATOR'S REPORT NUMBER(S) <b>ESD-TR-67-427</b>	
b. PROJECT NO. <b>7150</b>		9b. OTHER REPORT NO(S) (Any other numbers that may be assigned this report) <b>MTR-488</b>	
c.			
d.			
10. DISTRIBUTION STATEMENT <b>This document has been approved for public release and sale; its distribution is unlimited.</b>			
11. SUPPLEMENTARY NOTES <b>N/A</b>		12. SPONSORING MILITARY ACTIVITY <b>Development Engineering Division, Directorate of Planning and Technology, Electronic Systems Division, L. G. Hanscom Field, Bedford, Mass.</b>	
13. ABSTRACT <p>The loss in radar resolution, that is, the increase in mainlobe width and sidelobe level, has been computed for signals corrupted by a stationary random phase process. By making approximations appropriate to a coherent radar, an easily interpreted analysis is possible. The application to a CW radar or a pulsed radar using a reference oscillator with broadband phase errors is straightforward and indicates that a hash sidelobe level is introduced. A more general application, which corresponds to a crystal oscillator reference with narrowband phase errors requires the calculation of a convolution. Hash sidelobes are introduced in this case also, except that their level is a simple function of the ratio of the phase error and signal bandwidth.</p>			

## KEY WORDS

RADAR  
COHERENT RADAR  
RESOLUTION  
SIDELOBES

## LINK A

## LINK B

## LINK C

ROLE

WT

ROLE

WT

ROLE

WT